Thin-Walled Structures 87 (2015) 1–11

Contents lists available at ScienceDirect

Thin-Walled Structures

journal homepage: www.elsevier.com/locate/tws

Optimization of foam-filled double circular tubes under axial and oblique impact loading conditions

F. Djamaluddin, S. Abdullah *, A.K. Ariffin, Z.M. Nopiah

Department of Mechanical and Materials Engineering, Faculty of Engineering and Built Environment, Universiti Kebangsaan Malaysia, 43600 UKM Bangi, Selangor, Malaysia

ARTICLE INFO

Article history:
Received 17 April 2014
Received in revised form
9 October 2014
Accepted 30 October 2014

Keywords:
Aluminium foam
Crashworthiness
Cylindrical tube
Optimization
Oblique impact

ABSTRACT

This paper presents the multi objective optimization of foam-filled tubular tubes under pure axial and oblique impact loadings. In this work, the double circular tubes, whose bottom is the boundary condition, while at the top, is the impacted rigid wall; with respect to the axis of the tubes. The optimal crash parameter solutions, namely the minimum peak crushing force and the maximum specific energy absorption, are constructed by the Non-dominated Sorting Genetic Algorithm-II and the Radial Basis Function. Different configurations of structures, such as empty empty double tube (EET), foam filled empty double tube (FET), and foam filled foam filled double tube (FFT), are identified for their crashworthiness performance indicators. The results show that the optimal foam filled foam filled tube (FFT) had better crashworthiness than the others under pure axial loading. However, the foam filled empty tube (FET) was the best choice for structures under an oblique loading.

1. Introduction

One aim of the automotive industry is to increase the crashworthiness capability of structures and decrease weight for save fuel. Finding new materials and designs plays a major role in achieving this target. Simulated testing was chosen over physical testing due to cost. To improve the energy absorption of a material, thin-walled behaviour, which considered the parameters of geometry, size, cross-section, and loading conditions of the tubes, was studied [1,2]. The energy absorption behaviour of thin-walled circular tubes under axial impact has been studied by several scholars [1–5]. The dynamic instability of different cross-sections, such as circular and square tubes, subjected to axial impact loading, was reported in a book authored by Jones [2]. However, the progressive buckling, inversion, and splitting of circular tubes were previously discussed by [3]. Furthermore, Alghamdi et al. [4] studied the different structure's collapsibility as energy absorbers, namely circular and square tubes. Without increasing volume and weight too much, to improve the crashworthiness capability of thin-walled tubes, some researchers [6–11] used cellular materials, namely foams and honeycombs. The energy absorption capability of empty filled foam circular tubes, using a double-cell profile, was studied by Seitzberger et al. [12,13] and Nurick et al. [14].

In a real-world vehicle collapse event, thin-walled tubes work, not only with pure axial or pure bending loads, but also with a combination of axial and oblique loadings; particularly in a bumper system. The energy absorption capabilities of thin-walled tubes reduce more under a combination of axial and oblique impacts, compared to pure axial loads. The crush behaviour of mild steel square columns was analysed by Han and Park [15], indicating that from the axial to the bending collapse mode, there was a critical load angle at the transition place. Reyes et al. [16–19] studied square aluminium extrusion response, square tubes with and without foam, and circular tubes subjected to oblique loading, and obtained both experiment and simulation results. In addition, Li et al. [20] carried out deformation and energy absorption testing, using the experiment results for aluminium foam circular tubes, subjected to an oblique quasi-static loading. For tapered thin-walled rectangular tubes, Nagel and Thambiratnam [21–23] showed that this structure had more advantages than straight tubes under an oblique impact. In other types of structure, Ahmad et al. [24] also investigated the benefits of using foam-filled conical tubes under an oblique impact. Meanwhile, double circular tubes under axial and bending conditions using experimental and numerical testing were investigated by Guo et al. [25–28]. All gave good promising findings towards the development of crashworthiness properties.

* Corresponding author. Tel.: +60 3 89118411; fax: +60 3 89259659.
E-mail addresses: fauzan@siswa.ukm.edu.my (F. Djamaluddin), shahrum@eng.ukm.my (S. Abdullah), kamal@eng.ukm.my (A.K. Ariffin), zmn@eng.ukm.my (Z.M. Nopiah).

http://dx.doi.org/10.1016/j.tws.2014.10.015
0263-8231/

In recent years, concerns have increased on the optimization techniques applied to structural designs; especially to optimize the configurations of foam or cellular material filled thin-walled columns and tubes. For instance, maximizing energy absorption and minimizing the weight of foam filled [29,30] and honeycomb [31] under axial loads was investigated by Zarei and Kröger. In addition, multi objective optimization was used [32] to maximize specific energy absorption (SEA) and minimize the Peak Crushing Force (PCF) of honeycomb filled single and bitubular polygonal tubes. Aluminium foam filled-filled monotubal and bitubal thin walled square columns were optimized [33,34] using multi objective optimization. The results showed the foam-filled bitubal configuration to have more energy absorption efficiently than empty and its aluminium foam filler. Acar et al. [35] identified the maximum Crush Force Efficiency (CFE) and maximum SEA of tapered circular thin-walled tubes using multi objective crashworthiness optimization. The crashworthiness designs of empty and foam filled thin-walled square columns under an oblique impact loading were performed and indicated better outcomes [36]. Different mathematical programming was used to seek optimal solutions, such as genetic algorithms (GA) [37,33]. Sun et al. [38,39] used Particle Swarm Optimization (PSO) to optimize, with a two stage multi fidelity method for honeycomb, and optimized the crashworthiness design of Functionally Grade Foam (FGF) structures using Multi Objective Particle Swarm Optimization (MOPSO).

For all of the above mentioned studies, there was a limited concern about the foam-filled configuration of the double circular tube; particularly under different loading conditions. Furthermore, because of their good capability in energy absorption, these structures should be explored more, in order to gain an optimal design [20,28]. The aim of this current study paper is to optimize the crashing behaviour of double circular tubes under pure axial and oblique impact loadings using three different tubes, namely empty-empty double tube (EET), Foam-filled Empty Tube (FET), and Foam-Filled double Tube (FFT). In the design's problems, crashworthiness criteria i.e., SEA and PCF, were considered as design variables, such as diameter of cross-section, thickness, material, yield stress of wall, and the foam density. This work used s Non-dominated Sorting Genetic Algorithm (NSGA-II), due to the effectiveness of the crashworthiness design [40,41], to compare the optimal crashworthiness of the structures.

2. Materials and methods

2.1. Crashworthiness indicator of double tubes under axial and oblique impact loadings

To evaluate the energy-absorbance of structures, it is necessary to define the crashworthiness indicators. The parameters for instance Energy Absorption (EA), SEA, and PCF can efficiently evaluate the crashworthiness of structures. Energy absorption can be calculated as:

$$\mathrm{EA} = \int_0^{\delta} F(\delta)\,d\delta \tag{1}$$

where $F(\delta)$ is the instantaneous crashing force with a function of the displacement δ.

SEA indicates the absorbed energy (EA_{total}) per unit mass (M_{total}) of a structure as:

$$\mathrm{SEA} = \frac{\mathrm{EA}_{total}}{M_{total}} \tag{2}$$

where M_{total} is the structure's total mass. In this case, a higher value indicates the higher energy absorption efficiency of a material.

The average crush force (F_{avg}) is the response parameter for the energy absorption capability:

$$F_{avg} = \frac{\mathrm{EA}_{total}}{\delta} \tag{3}$$

where energy is absorbed (EA_{total}) during collapse and displacement (δ).

Crush force efficiency is defined as the ratio of the average crush force (F_{agv}) to the peak crush force (F_{max}),

$$\mathrm{CFE} = \frac{F_{avg}}{F_{max}} \tag{4}$$

Peak Crushing Force (PCF) is another important indicator in the design of energy absorption structures to absorb the impact energy in collision. When impact occurs i.e., automotive, PCF is able to determine the occupant's survival rate; therefore, several occupants injuries or even death [40] are caused by a large PCF.

2.2. Finite element models of the structures

Fig. 1 shows the schematic of the tubes under different impact loadings in particular axial (0°) and oblique (30°) impacts. The highest loading in mean force occurred at 30° without major reduction; this value was therefore chosen in the oblique impact [32,42,43]. To model energy absorbing structures, aluminium foam filled double tubes of length L=250 mm [32,34] were used to simulate the bumper beam of a passenger vehicle. Moreover, a stroke efficiency of 0.5 (as described by Chen et al. [44]) for all tubes was assumed at a maximum crash distance of 125 mm.

A rigid wall impacted the top of the tubes at an initial velocity of v=15 m/s. This speed was obtained from the New Car Assessment Program (NCAP). The rigid body was modelled as a mass block. All translational and rotational degrees of freedom were fixed and only translational displacement was allowed to move. Futhermore, the mass block of 110 kg was attached to the top free end. The bumper beam was assumed to absorb a kinetic energy of

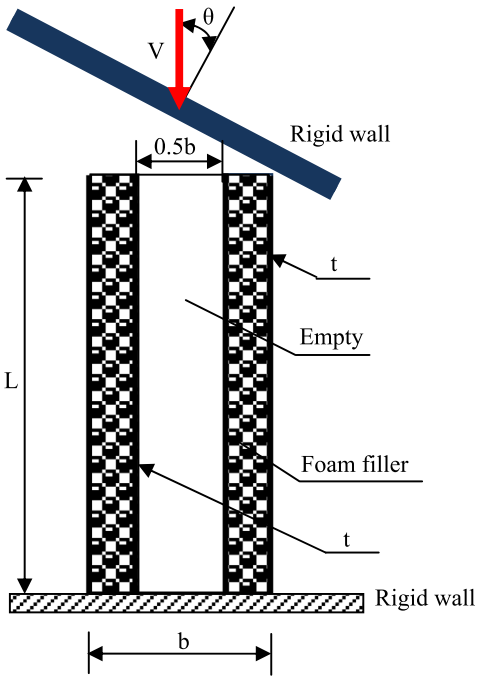

Fig. 1. Schematic of double circular tubes.

about 10% of the compact car's mass (about 1.100 kg) according to reference [45].

This material structure had a yield stress of aluminium thin-walled tubes σ_y and the density of foam filler ρ_f. The cross-section of the bitubal circular tubes is shown in Fig. 2. The outer diameter, b and the inner diameter, $0.5b$ of each tube measured 90 mm and 45 mm, respectively. The outer and inner thicknesses (t) of the double tube walls were the same at 1.8 mm.

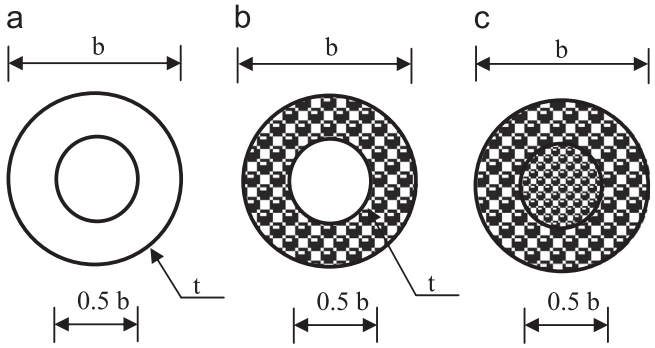

Fig. 2. Cross section of double circular tubes (a) empty-empty double tube (EET), (b) foam filled empty double tube (FET), and (c) foam filled-foam filled double Tube (FFT).

Fig. 3 shows the three FE models of Empty-Empty Tube (EET), empty-foam filled tube (FET), and foam filled-foam filled tube (FFT). Comparing the three double circular tubes with different configurations is important to design new bumper beam structures.

To develop the aluminium foam filled tubular tube models and to predict the response of thin walled structures impacted by a free falling impinging mass, the Finite Element (FE) code ABAQUS —Explicit was used.

The walls of the tubular tubes were modelled using four node shell continuum elements with five integration points along the element's thickness direction. Moreover, the foam filled tube was modelled using eight node continuum elements with a reduced integration technique combined with the hourglass control. To avoid both artificial zero energy deformation modes and volumetric locking, enhancement-based hourglass control and reduced integration were applied. Based on a mesh convergence study of shells and foam elements, a 2 mm element size was chosen. A mesh convergence was addressed to ensure a sufficient mesh density and to accurately capture the deformation process. The contact interaction between all components was the general contact algorithm used to avoid interpenetration of tube walls, which is less intense in terms of computational time. Meanwhile, the contacts between the foam and the tube walls were modelled as a finite sliding penalty based contact algorithm, with contact pairs and a hard contact. The friction coefficient value for all contact surfaces was set at 0.3 (as used in previous works [25,28]).

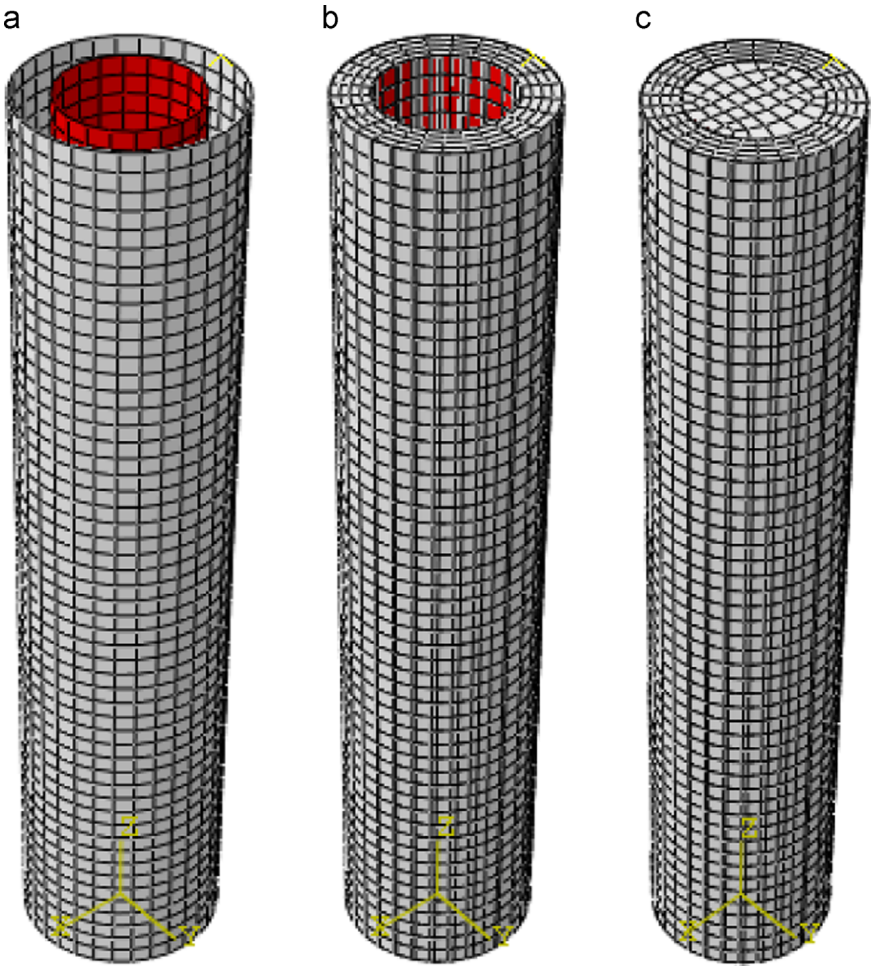

Fig. 3. The finite element model of cylindrical tubes. (a) EET, (b) FET and (c) FFT.

2.3. Material properties

2.3.1. Thin-walled circular double tubes material

The thin-walled tubes were made from aluminium alloy A6063 T6 [25,28] with mechanical properties of density $\rho=2700$ kg/m^3, the Young's modulus $E=60.2$ GPa, the Poisson's ratio $\nu=0.3$, initial yield stress $\sigma_y=184.4$ MPa, and ultimate stress $\sigma_u=215.5$ MPa.

The experiments showed that this structure had a much higher energy absorption and a steadier load carrying capacity than the single foam-filled tube under a bending condition [28]. Furthermore, for the experimental results of the cylinder tube structures under quasi-static oblique impact loading, the circular double tube had a greater energy absorption [20]. For these reasons, the double circular thin walled tubes were modified in an attempt to create the best structural model.

An elastic–plastic material model, with Von Mises's isotropic plasticity algorithm, was used to assess the constitutive behaviour of the tubes. The direction of aluminium foam, which caused manufacture process effect, was ignored. Piecewise lines were performed to define plastic hardening in the material's constitutive model. Moreover, the true stress and the plastic strain were experimentally found to determine the piecewise lines. For the uniaxial tension test results of the aluminium alloy A6063 T6 with different thicknesses, refer to Ref. [28]. The insensitivity of strain rate of aluminium alloy material [46], therefore the effect of strain rate in this model was omitted. This was because fracture of the aluminium alloy was not considered in the analysis.

2.3.2. Aluminium foam filled material

The aluminium closed-cell foam filler was used, with an average mechanical property value obtained from material tests. The material's behaviour was obtained from experimental testing of the foam filled material, while the uniaxial quasi-static compression test results with different foam apparent densities are given in references [25,28].

The constitutive behaviour was based on an isotropic uniform material of the foam model developed by Deshpande and Fleck [47] using non-linear ABAQUS/Explicit software packages. The effect of the manufacturing process for anisotropic behaviour of aluminium foam was not considered in this work. Table 1 shows the details of the material's parameters used in the FE simulation experiments.

The crushable foam and the crushable foam hardening options were used to calculate the plastic behaviour of the aluminium foam. The equation of yield criterion in this model is described as,

$$F=\hat{\sigma}-Y\leq 0 \tag{5}$$

where

$$\hat{\sigma}^2=\frac{1}{[1+(\alpha/3)^2]}\left[\sigma_e^2+\alpha\sigma_m^2\right] \tag{6}$$

where σ_e is the effective Von Mises stress and σ_m denotes the mean stress. The yield strength [48] is defined as Y. In addition, α is the parameter used to define the shape of the yield surface and the plastic coefficient function ν_p. It is assumed that the plastic Poisson's ratio for aluminium foam is zero [42,49]; thus, the formula is,

$$\alpha^2=\frac{2(1-2\nu_p)}{9(1+\nu_p)} \tag{7}$$

The strain hardening effect equation for the initial model is defined as,

$$Y=\sigma_p+\gamma\frac{\hat{\varepsilon}}{\varepsilon_D}+\alpha_2\ln\left[\frac{1}{1-(\hat{\varepsilon}/\varepsilon_D)^{\beta}}\right] \tag{8}$$

where σ_p is the plateau stress, the material constants are α_2, γ, ε_D and β, and the effective strain is defined as $\hat{\varepsilon}$. The strain of densification is derived as,

$$\varepsilon_D=-\frac{9+\sigma^2}{3\alpha^2}\ln\left(\frac{\rho_f}{\rho_{fo}}\right) \tag{9}$$

The density of foam and the base material is defined as ρ_f and ρ_{fo}, respectively [42,48].

Table 1
The parameters of the materials [25,28].

	ρg (cm^3)	E (Gpa)	ν	νp	k
Foam	0.45	0.625	0.1	0	1.732
Tube	2.7	60.2	0.3		

2.4. Design of experiment and metamodel technique

The DOE method provides the means to select the sampling points in the design space. Some design methods can be explored to sample points in the design space more efficiently [49,50]. To reduce the required sample number for constructing metamodels, crashworthiness performance was formulated using the D-optimal [51]. This method helped us to achieve a good quality metamodel [52]; the criterion of which offers a compromise between computational cost and accuracy [53].

Metamodel techniques are extensively used for design optimization to reduce computational costs. The most commonly used metamodels, which include the Polynomial Response Surface (PRS) models [54], Moving Least Square (MLS) [55], Artificial Neural Network (ANN) [56], Kriging [57], are used to calculate crashworthiness behaviour. The Radial Basis Functions (RBF) method was selected, because it indicates a fairly good accuracy for the global approximation of highly nonlinear responses and has been successfully used for previous crashworthiness optimizations [58–64]. Radial basis function was created by MATLAB in this work.

RBF was used as a surrogate model (metamodels) to represent the relationships between the individual objective functions and the design variable vector. Given the design variable vector and response values at n arbitrary design (training) points, the RBF approximation of the response function $f'(x)$ was derived from an FE simulation, as the following expression:

$$f'(x)=\sum_{i=1}^{n}\lambda_i\varnothing(||x-x_i||) \tag{10}$$

where x is the vector of the normalized design (input) variables with x_i representing the normalized coordinates of the i_{th} training point, $ri=||x-x_i||=\sqrt{((x-x_i)^T(x-x_i))}$, $\varnothing$ is a radial symmetric basis function, and $i=1$ is the unknown interpolation coefficients.

2.5. Multi objective optimization

The multi-objective optimization was explored with respect to the design variables of sectional diameter tubes, b; thickness of wall, t; yield stress, σ_y and foam density ρ_f, while the length of tube remained constant ($L=250$ mm).

Several works, [34,36,38,65–69], investigated two indicators of crashworthiness that could be optimized simultaneously. The main purpose of this study is to optimize aluminium foam-filled double tubes for maximum crashworthiness performance i.e., the maximum SEA and the minimum PCF, under axial and angle impact loadings. The multi-objective optimization scheme used

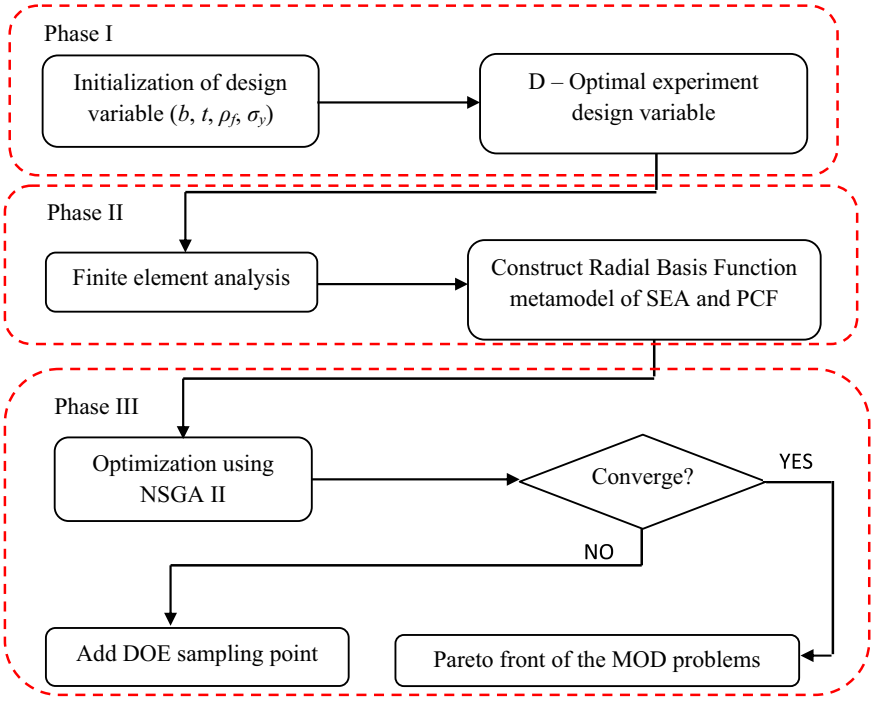

Fig. 4. Flowchart of crashworthiness multiobjective optimization for tubes.

Table 2
Difference between FE and experimental tests.

	Impact angle (°)	FE	Li ZB et al [20]	Error (%)
Energy Absorption (J)	0	3427.34	3524	2.74
Specific energy absorption (J/g)		25.93	26.7	2.88
Energy Absorption (J)	15	3197.28	3286	2.69
Specific energy absorption (J/g)		24.25	24.8	2.19

can be expressed mathematically as:

$$\begin{cases} Min\ F(x) = [f_1(y), f_2(y), \ldots, f_n(y)]^T \\ g_u(y) \geq 0, u = 1, \ldots, n \\ h_v(y) = 0, v = 1, \ldots, m \end{cases} \quad (11)$$

where y is the design variable vector, n is the objective function number, $f_n(y)$ is the objective function of the objective, $y^V = (y_1^V, y_2^V, \ldots y_1^V)$ denotes the lower bound, and $y^U = (y_1^U, y_2^U, \ldots y_1^U)$ the upper bound of the m design variables, and n and m are the numbers of unequal and equal constraints, respectively.

Genetic Algorithm (GA) is a popular optimization tool, because it avoids the trapping capability for searching for an optimum in local optima [70]. The Non-dominated Sorting GA (NSGA) algorithm, such as NSGA version I and II, are a more effective and efficient algorithm for ranking the solution, assigning ranking fitness, and benchmarking number problems [71].

The flowchart details for the crashworthiness optimization of double tubes under two impact loadings are shown in Fig. 4. First, the DoE method was used to define the design space and generate sampling points for different angle loadings (phase I). Second, FEA was used to acquire the design responses for the initial D-Optimal models of the design objectives (phase II). Finally, Pareto solutions of structures under different loading conditions used the NSGA II method (phase III).

3. Results and discussion

3.1. Model validation

Finite element models were compared to the experimental data based on the work by Li et al. [20] to ensure that they were sufficiently accurate for design optimization. The double circular aluminium foam tube model, subjected to oblique loading, was validated. The circular tube material was aluminium alloy AA6063 T6. In the experimental test [20], the double circular tube specimen was under a quasi-static oblique loading with a constant loading speed of 0.09 mm/s. The geometrics of the tube were length 90 mm, and outer and inner diameters of 38 mm and 24 mm, respectively. The thicknesses of the tube wall tube i.e., the inner and the outer, were 2.0 mm and 1.2 mm, respectively. Table 2 compares the FE experiment [20] under different angles of impact (0° and 15°) for double foam filled tube, found a good agreement for both results.

A radial basis functions metamodel was constructed to accurately sample points. To validate these models at a reasonable cost, five extra random points [34,36] were generated within the design domains of the six types of tubes subjected to the two specific load angles considered herein; which were 0° and 30°.

Both FE and RBF models were used to predict the responses (SEA and PCF) at these validation points. To measure the degree of approximation of the radial basis functions metamodel to the FEA results, the Relative Error (RE) [68] can be evaluated as:

$$RE = \left| \frac{y(x) - \tilde{y}(x)}{y(x)} \right| \quad (12)$$

where $\tilde{y}(x)$ is the radial basis functions models and $y(x)$ is the finite element result.

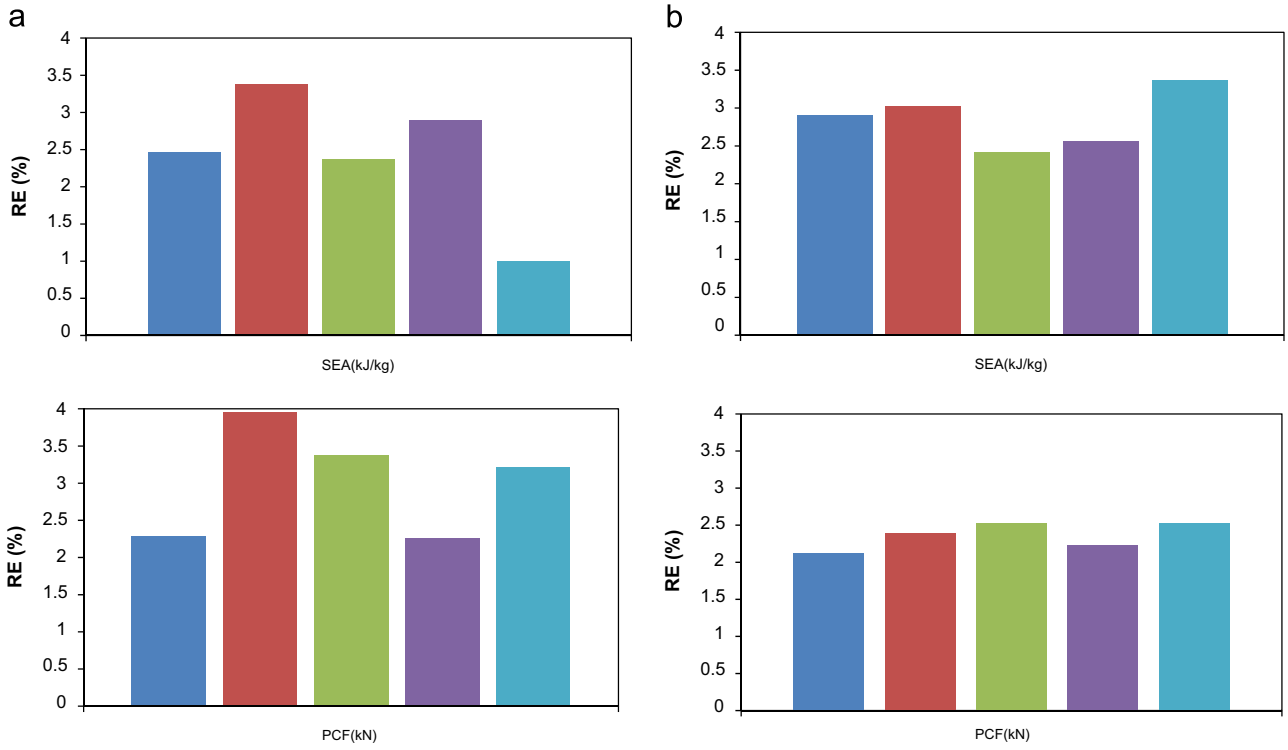

Fig. 5. Relative errors of design objectives of EET under (a) axial impact and (b) oblique impact.

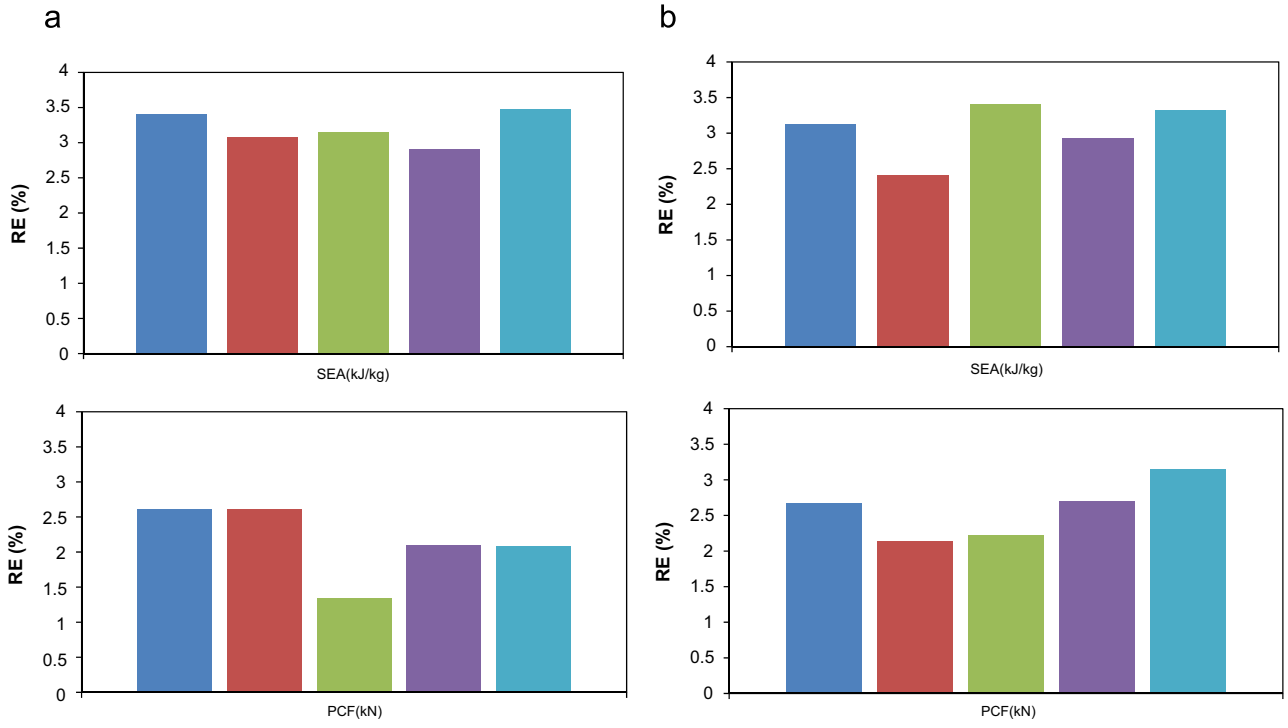

Fig. 6. Relative errors of design objectives of FET under (a) axial impact and (b) oblique impact.

Fig. 5 (EET), Fig. 6 (FET), and Fig. 7 (FFT), show the percentage of relative errors (% RE) of the initial sample points for the FEA and the RBF in five random sample points. The results show that the RE for these RBF metamodel approximations was less than 4%. Thus, it can be assumed that the RBF model for the objective functions (SEA and PCF) provided sufficient accuracy for design optimization.

3.2. Crashworthiness optimization design

The multi-objective optimization of aluminium foam double tube equations were derived by considering several parameters. Multi-objectives were applied when more than one objective existed and it needed to be used in the presence of trade-offs between two or more conflicting objectives. New objectives and

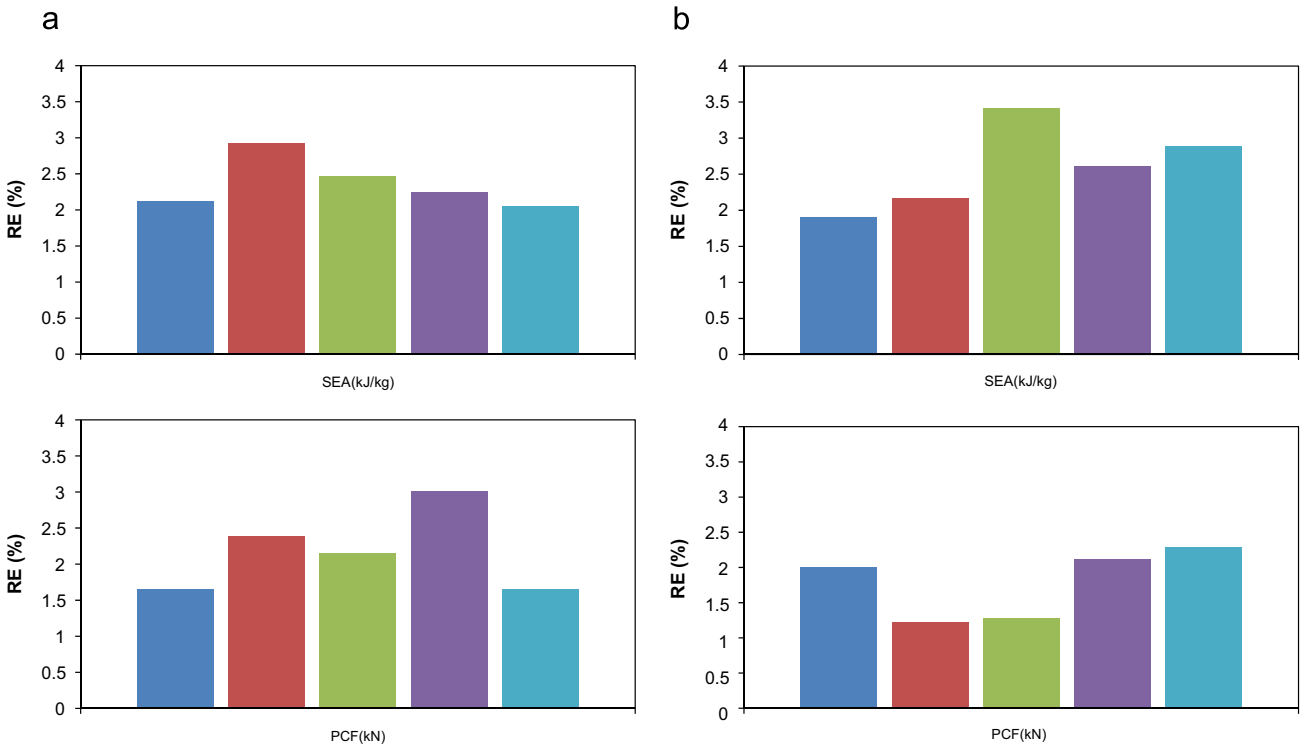

Fig. 7. Relative errors of design objectives of FFT under (a) axial impact and (b) oblique impact.

constraint functions, with respect to design variables, such as t, b, σ_y, ρ_f and objective functions, namely SEA and PCF for double circular tubes, were constructed (see Eqs. (13)–(15)).

Case one, the empty-empty double tube (EET). This tube condition was empty (ρ_f=0), with wall thickness (t), diameter (b), and wall material (σ_y) of bitubal tube. The design problem of optimization was defined as:

$$\begin{cases} \text{Min}\{-SEA(b,t,\ \sigma_y), \text{PCF}(b,t,\sigma_y)\} \\ 1.6\text{ mm} \le t \le 3.0\text{ mm} \\ s.t.\ 80\text{ mm} \le b \le 100\text{ mm} \\ 150\text{ MPa} \le \sigma_y \le 230\text{ MPa} \end{cases} \tag{13}$$

Case two, the foam filled empty double tube (FET). The double tubes, with empty and foam filled, with ρ_f as the foam density, were formulated as follows:

$$\begin{cases} \text{Min}\{-\text{SEA}(b,t,\rho_f,\sigma_y), \text{PCF}(b,t,\rho_f,\sigma_y)\} \\ 1.6\text{ mm} \le t \le 3.0\text{ mm} \\ s.t.\ 80\text{ mm} \le b \le 100\text{ mm} \\ 150\text{ MPa} \le \sigma_y \le 230\text{ MPa} \\ 110\text{ kg/m}^3 \le \rho_f \le 270\text{ kg/m}^3 \end{cases} \tag{14}$$

Case three, the foam filled–foam filled double tube (FFT). The formula is mathematically shown as:

$$\begin{cases} \text{Min}\{-\text{SEA}(b,t,\rho_f,\sigma_y), \text{PCF}(b,t,\rho_f,\sigma_y)\} \\ 1.6\text{ mm} \le t \le 3.0\text{ mm} \\ s.t.\ 80\text{ mm} \le b \le 100\text{ mm} \\ 150\text{ MPa} \le \sigma_y \le 230\text{ MPa} \\ 110\text{ kg/m}^3 \le \rho_f \le 270\text{ kg/m}^3 \end{cases} \tag{15}$$

The design variables, namely upper and lower bounds, were calculated by referring to the typical dimensions of a passenger car bumper beam in the literature [20,33,34].

MOD problems can be calculated to obtain the Pareto fronts (as shown in Eqs. (13)–(15)). Based on radial basis functions metamodels, the NSGA-II algorithm was adopted to investigate the design space. To create an initial 200 design point population for all cases of MOD, we used the DoE method. By considering the convergence of optimizations iterating for 20 generations, PCF vs.—SEA Pareto fronts graphs were generated using NSGA-II for EET, FET, and FFT tube structures. It was clear that they conflicted with each other in all SEA and PCF criteria design cases. Each double tube showed an increasing SEA, which led to undesirable PCF increases (as illustrated in Figs. 14 and 15).

3.3. Comparison of the structures under axial and oblique impact loadings

To compare the crashworthiness of the structures, a multi-objective optimization (as shown in Eqs. (13)–(15)), was used. All of the structures had similar dimensions, boundary, and loading conditions, as those considering the design variable (as shown in Fig. 1). The comparison of deformation patterns from the different structures can be seen. There were some progressive crease in the EET and FET (see Fig. 8a and b), while the FFT (Fig. 8c) indicated very limited expansion in the lateral direction.

The structures under oblique impact (Fig. 9) revealed that the FET (Fig. 9b) can withstand more than EET and FFT (Fig. 9a and c). Due to the comparison of different concept designs, the energy absorption was plotted to the deformation of the length of tubes. Moreover, as a function of deformation, the energy absorption was plotted to simplify the comparison of structure configuration design concepts.

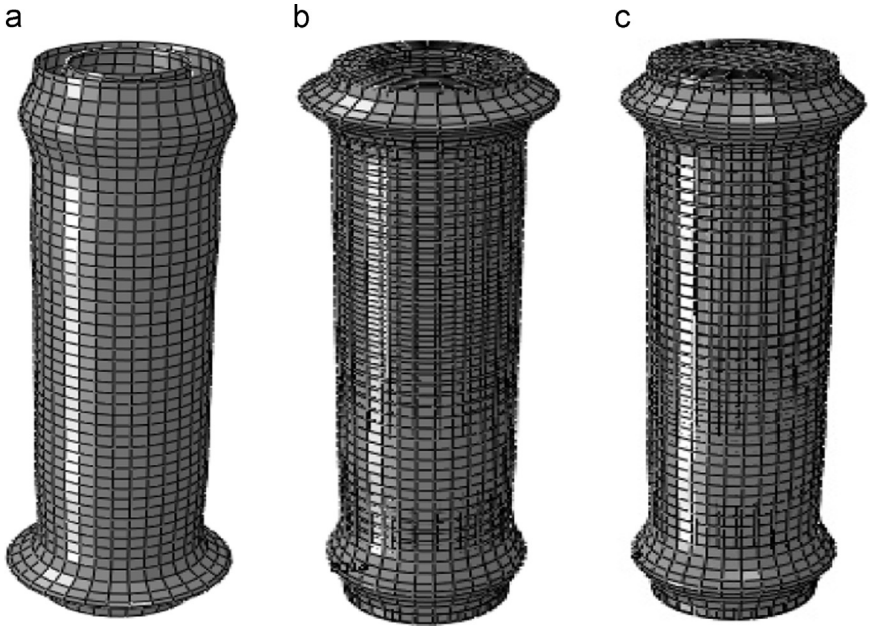

Fig. 8. Deformation modes of (a) FFT, (b) FET and (c) EET under pure axial impact loading.

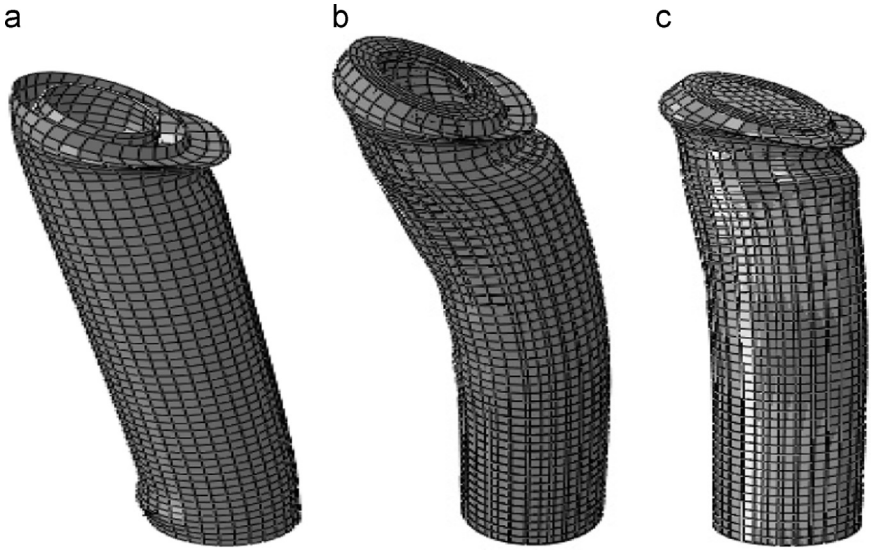

Fig. 9. Deformation modes of (a) FFT, (b) FET and (c) EET under oblique impact loading.

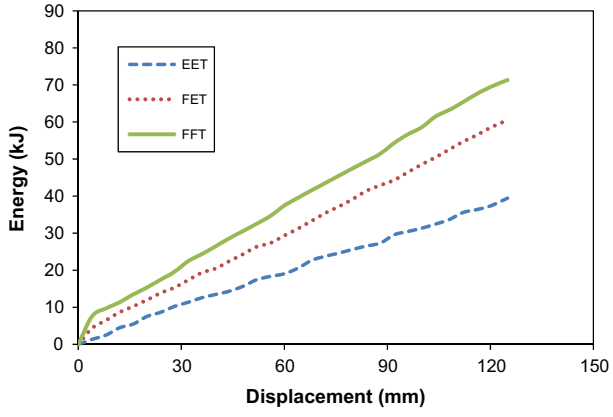

Fig. 10. Energy absorbtion capability for various structures of the foam filler double tube under pure axial loading.

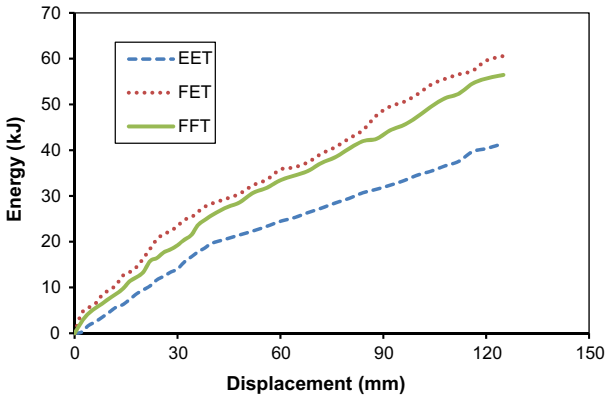

Fig. 11. Energy absorption capability for various structures of the foam filler double tube under oblique loading.

Table 3
Optimal designs for three structures.

Impact angle	Double tubes	Objective function	b (mm)	t (mm)	σ_y (MPa)	ρ_f (kg/m^3)	SEA (kJ/kg)	PCF (kN)
0	EET	SEA	87.43	2.451	197.54	–	**16.64**	158.87
		PCF	85.61	2.345	210.63	–	4.78	**63.54**
	FET	SEA	87.59	2.643	200.73	206.74	**18.57**	163.23
		PCF	86.78	2.943	199.32	154.75	5.48	**75.12**
	FFT	SEA	90.21	2.230	198.97	203.89	**19.98**	172.49
		PCF	87.02	2.753	209.45	146.32	6.43	**83.43**
30	EET	SEA	87.43	2.102	203.76	–	**8.83**	66.23
		PCF	86.31	2.451	208.81	–	2.86	**30.85**
	FET	SEA	89.92	2.991	208.34	205.38	**10.16**	81.09
		PCF	87.44	2.459	205.62	169.21	3.98	**47.54**
	FFT	SEA	90.23	2.145	201.54	219.65	**9.82**	73.94
		PCF	89.45	2.751	206.69	178.42	4.64	**39.3**

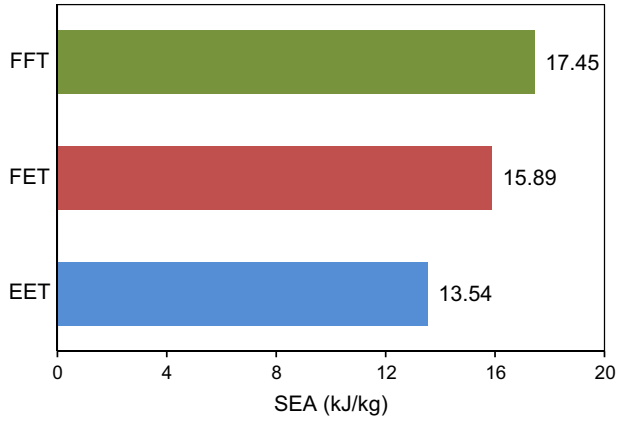

Fig. 12. Specific energy absorption for various structures of the foam filler double circular tubes under pure axial impact.

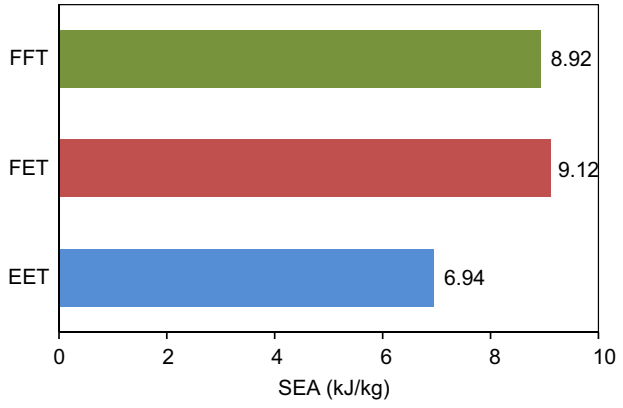

Fig. 13. Specific energy absorption for various structures of the foam filler double circular tubes under oblique impact.

Figs. 10 and 11 show that FET and FFT were better energy absorbers in both loading conditions. It can be seen that the EET geometry had lower energy absorption than other configuration structures under axial and oblique loadings. However, the combination structures i.e., FET and FFT had more energy absorption capacity and lower peak crushing force, due to the frictional interaction between the foam-filler and the inner/outer tubes [34,72]. These structures will therefore be able to improve the crashworthiness performance of thin-walled tubes; especially in vehicle design.

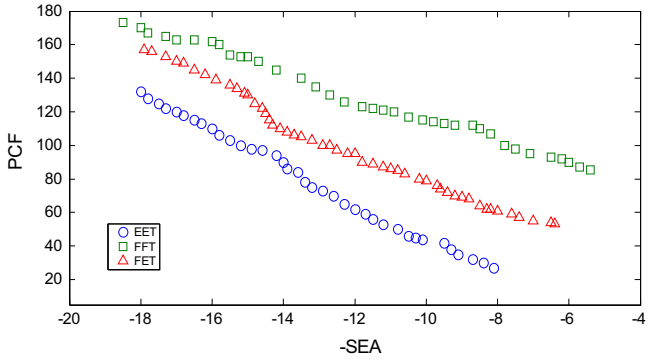

Fig. 14. Pareto fronts for various structures of foam filler double tubes under pure axial loading.

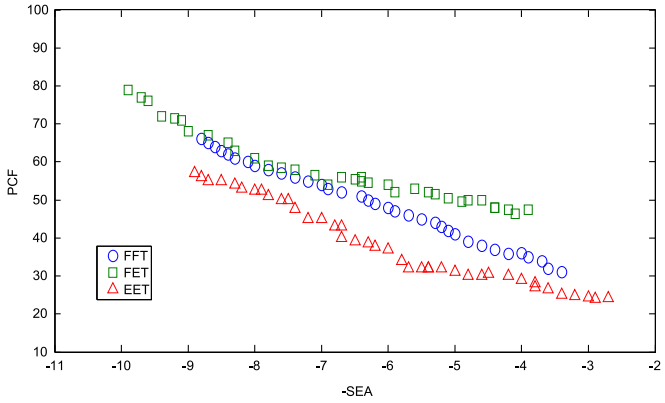

Fig. 15. Pareto fronts for various structures of foam filler double tubes under oblique loading.

Table 3 lists the optimal configurations of EET (columns 4–6), FET (columns 4–7), and FFT (columns 4–7) under both loading conditions, and the ideal optimal values for two single objective functions, SEA (column 8) and PCF (column 9). For each of the structure designs in this table, first the maximum SEA is 19.98 kJ/kg when FFT was under pure axial impact. It is preferable that the wall has a thickness value of 2.230 mm and material yield stress of 203.89 MPa, while for the minimization of PCF at EET under 30° with wall thickness lower bounds of 2.451 mm and yield stress of 208.81 MPa. This is evidence that there is a confliction between the two objective functions of the crashworthiness and the verification applied multi objective optimization in such problems. Second, the optimal diameter of each circular double tube for maximum SEA is generally different under both impact conditions. For instance, the diameter of the optimal section of FFT under pure axial impact for maximum SEA was 85.61 mm, while in the same objective under 30°, it was 90.23 mm. In these two cases, the corresponding optimal values for FET were 87.54 mm and 88.92 mm, respectively. Apparently, the large diameter tube gave the effect of energy absorption with a constant tube length. Thus, yield wall of tube material more susceptible to deform structures and more energy efficient progressive collapse mode under oblique impact. However, increasing mass with a large tube diameter effects reducing SEA. Finally, foam-filler tubes of the minimum PCF were close to lower bond of 146.32 kg/m^3 for both impact angles. The optimum value to maximize SEA was found to be the highest foam density of 219.65 kg/m^3 when the circular double tube was impacted at a 30° angle. However, the optimal foam density of the SEA maximization lowers under pure axial impact more than oblique impact, as seen in reference [33,36], also are shown in Figs. 12 and 13).

Multi-objective optimization was explored with respect to the design variables of sectional diameter tubes, *b;* thickness, *t;* yield stress, σ_y and foam density ρ_f. In addition, five random sample points [36] were considered to define the errors between the FEA and the radial basis functions models. The circular double tubes Pareto fronts can be plotted (see Figs. 14 and 15) using the radial basis functions and NSGA-II optimization method. In this section, EET, FET, and FFT were optimized under 0° and 30° as pure axial and oblique loading conditions. For the entry of foam-filler in the crashworthiness simulation, the corresponding MOD problems and RBF models were implied.

4. Conclusions

The crashworthiness design for thin-walled structures made of aluminium foam filled circular tubes was explored in this paper. Crashworthiness criteria, such as specific energy absorption (SEA) and Peak Crushing Force (PCF) were calculated under axial and oblique impact loadings. Multi objective problems based on Radial Basis Functions (RBF) were constructed using Finite Element Analysis (FEA). As a result, the maximum SEA and the minimum PCF under pure axial loading conditions were 19.98 kJ/kg and 63.54 kN, respectively. Similarly, the value under an impact angle of 30° obtained the maximum value of SEA at 10.16 kJ/kg and the minimum PCF of 30.85 kJ/kg. Normally, it was found that increasing the angle of loading on the double circular tubes led to a decrease in the values of SEA and PCF.

The main result can be described as follows: first, Non-dominated Sorting Genetic Algorithm-II (NSGA-II) was used for the multi-objective optimization of SEA and PCF for circular double tubes. Second, to optimize the different double tube structures, namely empty-empty double tube (EET), foam filled-empty double tube (FET), and foam filled-foam filled double tube (FFT). Third, results comparison showed that FFT crashworthiness performed about 12% better than the others structures (i.e., EET and FET) for pure axial impact. To compare structures under an oblique impact of 30°, the results demonstrated that FET of was the best choice, about 7% for the SEA better than FFT. The FET and FFT were good potential candidates for energy absorbing crashworthiness structure applications, to protect vehicle occupants during accidents or collisions.

References

[1] Lu G, Yu T. Energy absorption of structures and materials. Woodhead Publishing Limited; 2003.
[2] Jones N. Structural impact. Cambridge University Press; 1989.
[3] Reid SR. Plastic deformation mechanisms in axial compressed metal tubes used as impact energy absorbers. Int J Mech Sci 1993;35(12):1035–52.
[4] Alghamdi AAA. Collapsible impact energy absorbers: an overview. Thin Walled Struct 2001;39(2):189–213.
[5] Alexander JM. An approximate analysis of the collapse of thin cylindrical shells under axial loading. Q J Mech Appl Math 1960;13:10–5.
[6] Hanssen AG, Langseth M, Hopperstad OS. Static crushing of square aluminium extrusions with aluminium foam filler. Int J Mech Sci 1999;41(8):967–93.
[7] Hanssen AG, Langseth M, Hopperstad OS. Axial crushing of aluminium columns with aluminium foam filler. In: Proceedings of the seventh international symposium on structural failure and plasticity (IMPLAST2000); 2000. p. 401–7.
[8] Hopperstad OS, Langseth M, Hanssen AG. Static and dynamic crushing of circular aluminium extrusions with aluminium foam filler. Int J Impact Eng 2000;24(5):475–507.
[9] Hopperstad OS, Langseth M, Hanssen AG. Optimum design for energy absorption of square aluminium columns with aluminium foam filler. Int J Mech Sci 2001;43(1):153–76.
[10] Santosa SP, Wierzbicki T, Hanssen AG, Langseth M. Experimental and numerical studies of foam-filled sections. Int J Impact Eng 2000;24(5):509–34.
[11] Thornton PH. Energy absorption by foam filled structures. SAE paper 800081; 2005.
[12] Seitzberger M, Rammerstorfer RF, Degischer HP, Gradinger R. Crushing of axially compressed steel tubes filled with aluminium foam. Acta Mech 1997;125:93–105.
[13] Seitzberger M, Rammerstorfer FG, Gradinger R, Degischer HP, Blaimschein M, Walch C. Experimental studies on the quasi-static axial crushing of steel columns filled with aluminium foam. Int J Solids Struct 2000;37(30):4125–47.
[14] Yuen S, Kim Chung, Nurick GN, Starke RA. The energy absorption characteristics of double-cell tubular profiles. Lat Am J Solids Struct 2008;5(4):289–317.
[15] Han DC, Park SH. Collapse behavior of square thin-walled columns subjected to oblique loads. Thin-walled Struct 1999;35:167–84.
[16] Reyes A, Langseth M, Hopperstad OS. Crashworthiness of aluminum extrusions subjected to oblique loading: experiments and numerical analyses. Int J Mech Sci 2002;44(9):1965–84.
[17] Reyes A, Langseth M, Hopperstad OS. Square aluminum tubes subjected to oblique loading. Int J Impact Eng 2003;28(10):1077–106.
[18] Børvik T, Hopperstad OS, Reyes A, Langseth M, Solomos G, Dyngeland T. Empty and foam-filled circular aluminium tubes subjected to axial and oblique quasi-static loading. Int J Crashworthiness 2003;8(5):481–94.
[19] Reyes A, Hopperstad OS, Langseth M. Aluminum foam-filled extrusions subjected to oblique loading: experimental and numerical study. Int J Solids Struct 2004;41(5–6):1645–75.
[20] Li ZB, Yu JL, Guo LW. Deformation and energy absorption of aluminum foam-filled tubes subjected to oblique loading. Int J Mech Sci 2012:48–56.
[21] Nagel G, Thambiratnam D. A numerical study on the impact response and energy absorption of tapered thin-walled tubes. Int J Mech Sci 2004;46:201–16.
[22] Nagel G, Thambiratnam D. Computer simulation and energy absorption of tapered thin-walled rectangular tubes. Thin-Wall Struct 2005;43:1225–42.
[23] Nagel G, Thambiratnam D. Dynamic simulation and energy absorption of tapered thin-walled tubes under oblique impact loading. Int J Impact Eng 2006;32:1595–620.
[24] Ahmad Z, Thambiratnam DP, Tan ACC. Dynamic energy absorption characteristics of foam-filled conical tubes under oblique impact loading. Int J Impact Eng 2010;37:475–88.
[25] Guo LW, Yu JL. Bending behavior of aluminum foam-filled double cylindrical tubes. Acta Mech 2011;222:233–44.
[26] Guo LW, Yu JL. Bending response of sandwiched double tube structures with aluminum foam core. In: Lu JWZ, Leung AYT, Iu VP, Mok KM, editors.. Proceedings of the ISCM II & EPMESC XII, Hong Kong-Macau, 2009. AIP CP1233, Part One. Melville, New York: American Institute of Physics; 2010. p. 602–607.
[27] Guo LW, Yu JL. Experimental studies on the quasi-static axial crushing behavior of double square columns filled with aluminum foams. J Exp Mech 2010;25(3):271–8 ([in Chinese]).
[28] Guo LW, Yu JL. Dynamic bending response of double cylindrical tubes filled with aluminum foam. Int J Impact Eng 2011;38(2–3):85–94.
[29] Zarei HR, Kröger M. Optimization of the foam-filled aluminum tubes for crush box application. Thin-Wall Struct 2008;46:214–21.
[30] Zarei HR, Kröger M. Bending behavior of empty and foam-filled beams: structural optimization. Int J Impact Eng 2008;35:521–9.
[31] Zarei H, Kröger M. Optimum honeycomb filled crash absorber design. Mater Des 2008;29:193–204.
[32] Yin H, Wen G, Hou S, Chen K. Crushing analysis and multiobjective crashworthiness optimization of honeycomb-filled single and bitubular polygonal tubes. Mater Des 2011;32:4449–60.
[33] Hou S, Li Q, Long S, Yang X, Li W. Crashworthiness design for foam filled thin-wall structures. Mater Des 2009;30:2024–32.
[34] Zhang Y, Sun G, Li G, Luo Z, Li Q. Optimization of foam-filled bitubal structures for crashworthiness criteria. Mater Des 2012;38:99–109.
[35] Acar E, Guler MA, Gerçeker B, Cerit ME, Bayram B. Multi-objective crashworthiness optimization of tapered thin-walled tubes with axisymmetric indentations. Thin-Wall Struct 2011;49:94–105.
[36] Yang S, Qi C. Multiobjective optimization for empty and foam-filled square columns under oblique impact loading. Int J Impact Eng 2013:177–91.
[37] Nariman-Zadeh N, Darvizeh A, Jamali A. Pareto optimization of energy absorption of square aluminium columns using multi-objective genetic algorithms. Proc Inst Mech Eng Part B J Eng Manuf 2006;220:213–24.
[38] Sun GY, Li GY, Stone M, Li Q. Application two-stage multi-fidelity optimization procedure for honeycomb-type. Comput Mater Sci 2010;49:500–11.
[39] Sun GY, Li GY, Hou SJ, Zhou SW, Li W, Li Q. Crashworthiness design for functionally graded foam filled thin-walled structures. Mater Sci Eng, A 2010;527:1911–9.
[40] Liao XT, Li Q, Yang XJ, Li W, Zhang WG. A two-stage multiobjective optimization of vehicle crashworthiness under frontal impact. Int J Crashworthiness 2008;13:279–88.
[41] Liao XT, Li Q, Zhang WG, Yang XJ. Multiobjective optimization for crash safety design of vehicle using stepwise regression model. Struct Multidisciplinary Optim 2008;35:561–9.
[42] Ahmad Z, Thambiratnam DP. Dynamic computer simulation and energy absorption of foam-filled conical tubes under axial impact loading. Comput Struct 2009;87(3–4):186–97.
[43] Tarlochan F, Samerb F, Hamoudac AMS, Rameshd S, Karam K. Design of thin wall structures for energy absorption applications: enhancement of crashworthiness due to axial and oblique impact forces. Thin Walled Struct 2013;71:7–17.

[44] Chen WG, Wierzbicki T. Relative merits of single-cell, multi-cell and foam filled thin-walled structures in energy absorption. Thin Walled Struct 2001;39:287–306.
[45] Witteman WJ. Improved vehicle crashworthiness design by control of the energy absorption for different collisions situation. Netherlands: Eindhoven University of Technology; 1999 (PhD thesis).
[46] Langseth M, Hopperstad OS. Static and dynamic axial crushing of square thin-walled aluminium extrusions. Int J Impact Eng 1996;18:949–68.
[47] Deshpande VS, Fleck NA. Isotropic constitutive models for metallic foams. J Mech Phys Solids 2000;48:1253–83.
[48] Shahbeyk S, Spetrinic N, Vafai A. Numerical modelling of dynamically loaded metal foam-filled square columns. Int J Impact Eng 2007;34:573–86.
[49] Reyes A, Hopperstad OS, Berstad T, Hanssen AG, Langseth M. Constitutive modeling of aluminum foam including fracture and statistical variation of density. Eur J Mech A: Solids 2003;22(6):815–35.
[50] Kleijnen JPC. An overview of the design and analysis of simulation experiments for sensitivity analysis. Eur J Oper Res 2005;164(2):287–300.
[51] Song XG, Sun GY, Li GY, Gao WZ, Li Q. Crashworthiness optimization design of foam-filled tapered thin-walled structures using multiple surrogate models. Struct Multidisciplinary Optim 2013;47(2):221–31.
[52] Myers RH, Montgomery DC. Response surface methodology: process and product optimization using designed experiments. New York: Wiley; 1995.
[53] Redhe M, Forsberge J, Janssone T, Marklund PO, Nilsson L. Using the response surface methodology and the D-optimality criterion in crashworthiness related problems an analysis of the surface approximation error versus the number of function evaluations. Struct Multidisciplinary Optim 2002;24:185–94.
[54] Roux W. Structural optimization using response surface approximations. PhD thesis, University of Pretoria, 1997.
[55] Myers RH, Montgomery DC. Response surface methodology: process and product optimization using designed experiments. New York: Wiley; 1995.
[56] Lancaster P, Salkauskas K. Surfaces generated by moving least square methods. Math Comput 1981;37:141–58.
[57] Ding S, Li H, Su C, Yu J, Jin F. Evolutionary artificial neural networks: a review. Artif Intell Rev 2011:1–10.
[58] Acar E, Rais-Rohani M. Ensemble of metamodels with optimized weight factors. Struct Multidisciplinary Optim 2008;37:279–94.
[59] Rais-Rohani M, Singh MN. Comparison of global and local response surface techniques in reliability-based optimization of composite structures. Struct Multidisciplinary Optim 2003;26:333–45.
[60] Fang H, Rais-Rohani M, Liu Z, Horstemeyer MF. A comparative study of metamodeling methods for multiobjective crashworthiness optimization. Comput Struct 2005;85:2121–36.
[61] Chang Q, Shu Y, Fangliang D. Crushing analysis and multiobjective crashworthiness optimization of tapered square tubes under oblique impact loading. Thin-Walled Struct 2012;59:103–19.
[62] Fang H, Wang Q. On the effectiveness of assessing model accuracy at design points for radial basis functions. Commun Numer Methods Eng 2008;24:219–35.
[63] Salehghaffari S, Rais-Rohani M, Anajafi. Analysis and optimization of externally stiffened crush tubes. Thin-Walled Struct 2011;49:397–408.
[64] Hou S, Li Q, Long S, Yang X, Li W. Crashworthiness design for foam filled thin-wall structures. Mater Des 2009;30:2024–32.
[65] Yin H, Wen G, Liu Z, Qing Q. Crashworthiness optimization design for foam-filled multi-cell thin-walled structures. Thin-Walled Struct 2014;75:8–17.
[66] Franulovic M, Basan R, Prebil I. Genetic algorithm in material model parameters identification for low-cycle fatique. Comput Mater Sci 2009;75:505–10.
[67] Zhang Y, Sun G, Xu X, Li G, Li Q. Multiobjective crashworthiness optimization of hollow and conical tubes for multiple load cases. Thin-Walled Struct 2014;82:331–42.
[68] Fang J, Gao Y, Sun G, Zhang Y, Li Q. Crashworthiness design of foam-filled bitubal structures with uncertainty. Int J Linear Mech 2014.
[69] Yin H, Wen G, Fang H, Qing Q, Kong X, Xiao J, et al. Multiobjective crashworthiness optimization design of functionally graded foam-filled tapered tube based on dynamic ensemble metamodel. Mater Des 2014;55:747–57.
[70] Murugan P, Kannan S, Baskar S. NGSA-II algorithm in for multiobjectiv evgeneration expansion planning problem. Eletric Power Syst Res 2009;79:622–8.
[71] Deb K. Multiobjective optimization using evolutionary algorithms. John Wiley & Sons; 2001.
[72] Othman A, Abdullah A, Ariffin AK, Mohamed NAN. Investigating the quasi-static axial crushing behavior of polymeric foam-filled composite pultrusion square tubes. Mater Des 2014;632:446–59.